AIMS Materials Science, 2(4): 356-368.
DOI: 10.3934/matersci.2015.4.356
Received date 19 May 2015,
Accepted date 16 September 2015,
Published date 08 October 2015

http://www.aimspress.com/

Research article

Quantitative characterization and modeling of sub-bandgap absorption features in thin oxide films from spectroscopic ellipsometry data

Dmitriy V. Likhachev [1,*], Natalia Malkova [2], and Leonid Poslavsky [2]

[1] GLOBALFOUNDRIES Dresden Module One LLC & Co. KG, Wilschdorfer Landstr. 101, D-01109 Dresden, Germany
[2] KLA-Tencor Corp., One Technology Drive, Milpitas, CA 95035, U.S.A.

* **Correspondence:** Email: dmitriy.likhachev@globalfoundries.com; Tel: +49-351-277-7911; Fax: +49-351-277-97911.

Abstract: Analytic representations of the complex dielectric function, which describe various types of materials, are needed for the analysis of optical measurements, in particularly, ellipsometric data. Here, we examine an improved multi-oscillator Tauc-Lorentz (TL) model with a constraint on the band-gap parameter E_g, which forces it to be common for all TL oscillators, and possibility to represent reasonably weak absorption features below the bandgap by inclusion of additional unbounded Lorentz and/or Gaussian oscillators with transition energies located below E_g. We conclude that the proposed model is the most appropriate for the characterization of various materials with sub-band absorption features and provides meaningful value for the energy bandgap. A few examples to illustrate the use of modified model have been provided.

Keywords: thin oxide films; optical characterization; spectroscopic ellipsometry; optical constants; dielectric function; parameterization; optical modeling; optical metrology

1. Introduction

The global trend of miniaturization in modern semiconductor manufacturing continues to stimulate new applications of spectroscopic ellipsometry (SE). For instance, the presence of electrically active defects in thin oxide layers of semiconductor devices limits their performance and reliability. In recent years, a few papers were dedicated to application of spectroscopic ellipsometry to diagnose and characterize charge trapping defects in thin dielectric film stacks [1–10]. Indeed,

spectroscopic ellipsometry, as well-established and widely used in-line characterization technique in semiconductor volume manufacturing, can provide one of the ways to monitor noninvasively the presence of dislocations and defects in large densities during semiconductor device fabrication.

Meanwhile, SE has an *indirect* nature and requires appropriate modeling analysis to interpret optical measurements and extract useful information. In particular, this analysis demands a suitable optical model consisted of the optical properties of materials (the complex refractive index $N = n + ik$ or the dielectric function $\varepsilon = \varepsilon_1 + i\varepsilon_2$) and thickness (or other topographic parameters) of each layer for a structure under investigation. In the simplest case, tabulated data for the *n*&*k*'s of each layer can be used as inputs for the optical model. On the one hand, this assumption may seem natural and advantageous since it does not overcomplicate the model. However, in practice, even relatively small deviations in material optical properties (from nominal model inputs) due to process condition variations may significantly affect the measurement results. Moreover, the material optical properties might be unknown *a priori* and need to be determined during characterization. In that situation, when the optical constants are not really "constant", i.e., fixed and invariable, and/or not established beforehand, modeling or parameterization of the material *n*&*k*'s becomes an absolute necessity [11–13] and for this purpose many analytical physics-based and Kramers–Kronig consistent expressions (models) have been developed which describe various types of materials—amorphous and crystalline semiconductors and dielectrics, metals, organic films, optical metamaterials, etc.

However, in some cases current parametric models cannot be used adequately since they do not account for discrete absorption features below the bandgap which can be associated with defects or film structural changes [1,5,7,14,15]. Instead, one can use so-called "point-by-point data inversion" method (also known as "direct data inversion" or "exact numerical inversion") to represent the dielectric function. In a point-by-point inversion procedure the *n*&*k*'s dependency on each other at different wavelengths is disregarded, all variables in the optical model are fixed except the *n*&*k* values for analyzable material at each wavelength λ (or ε_1 and ε_2, i.e., the real and imaginary part of the dielectric function at each photon energy E) and values for n and k at each wavelength are calculated from the measured ellipsometric parameters Psi (Ψ) and Delta (Δ). Obviously, the point-by-point method should be used with great caution. First of all, the correct initial model must be used for such direct data inversion, i.e., all other parameters, except the *n*&*k* values for the material under study, need to be known with high accuracy, otherwise those modeling errors can lead to unphysical dispersion or discontinuities in the optical constants. Moreover, existing measurement noise will be directly translated into extracted *n*&*k* values. Even more importantly, the method does not enforce Kramers–Kronig consistency between the real and imaginary part of the obtained optical constants (or, dielectric function) and, therefore, can result in unphysical shape of the (n,k)-curve in the considered spectral range. Of course, this approach is not appropriate for all applications and the physics-based oscillator models with physically meaningful parameters should still be preferable since they can provide further insights into other important material properties such as composition, phase structure, doping, stress, uniformity, electrical properties, etc.

Almost 20 years ago, Jellison, Jr. and Modine suggested new optical function parameterization, namely so-called Tauc–Lorentz (TL) oscillator model [16], which quickly became very popular parameterization for the dielectric functions of amorphous semiconductors and dielectrics. Original version of the model was proposed for single interband transition, i.e., the imaginary part of the dielectric function ε_2 near the band edge was expressed as single TL oscillator:

$$\varepsilon_2(E) = \begin{cases} \dfrac{AE_0C(E-E_g)^2}{(E^2-E_0^2)^2+C^2E^2}\dfrac{1}{E}, & E > E_g, \\ 0, & E \le E_g, \end{cases} \tag{1}$$

where E_g is the bandgap of the material, A is the oscillator amplitude, E_0 is the energy (position) of the Lorentz peak, and C is the broadening parameter. Nevertheless, very often in practice it is necessary to generalize the model for a case of multiple TL oscillators to describe more accurately the optical properties of various materials. But more often than not these multi-oscillator implementations incorporate *different* band-gap parameters E_g and, therefore, violate a physicality of the dispersion model which assumes a uniqueness requirement for the band-gap value.

Here we apply a modified Tauc-Lorentz dispersion model with common band-gap parameter E_g and possibility to represent reasonably the absorption features below the bandgap. We illustrate our approach with a few examples of the dielectric function parameterization. These examples have been selected for their relevance to some practical circumstances in material characterization for modern technological applications. We expect that this approach will increase the accuracy of estimation of the optical functions to meet the needs in many practical situations in the microelectronic industry.

2. Model Description

A well-known problem with the application of the TL model to thin films is that it explicitly neglects the absorption below E_g, i.e., $\varepsilon_2(E) = 0$ for $E \le E_g$, which makes the modeling of the optical spectra for some materials in the vicinity of the absorption edge problematic [15]. Typically, the sub-band absorption is modeled by combining the exponential Urbach tail

$$\varepsilon_2(E) = \frac{E_1}{E}\exp\left\{\frac{E-E_t}{E_u}\right\} \qquad (0 < E \le E_t), \tag{2}$$

where E_t denotes the demarcation energy between the Urbach tail transitions and the interband transitions and E_u is the so-called Urbach energy, representing the width of tail states in the forbidden gap, with the TL oscillator [17–20]. In some cases, this approach demonstrated an improved description of the optical dielectric response for the materials such as, for example, high-κ dielectric films [15,21,22], hydrogenated amorphous silicon nitride (a-SiN_x:H) films [23] and titanium dioxide (TiO_2) thin films [24,25]. However, the absorption below the band gap often does not correspond to the Urbach tail and the simple combination of Eq. (2) with the TL oscillator(s) is insufficient. In our approach, the imaginary part of dielectric function ε_2 includes not only the TL oscillator(s) with $E_{0j} > E_g$ but also an ensemble of free/unbounded Lorentz and/or Gaussian oscillators. Importantly, the band-gap parameter E_g is set to be the same for all TL oscillators. Thus, the imaginary part of the dielectric function ε_2 in TLLG model is defined as follows:

$$\varepsilon_2(E) = G_T(E)L_b(E) + L_f(E) + G_f(E), \tag{3}$$

where $G_T(E)$ in the first term represents the Tauc gap function

$$G_T(E) = \begin{cases} \dfrac{(E-E_g)^2}{E^2}, & E > E_g, \\ 0, & E \le E_g, \end{cases} \tag{4}$$

$L_b(E)$ and $L_f(E)$ are set as the sum of the bounded or free/unbounded Lorentz oscillators

$$L_{(b,f)}(E) = \sum_j \frac{A_j E_{0j} C_j^2 E}{(E^2 - E_{0j}^2)^2 + C_j^2 E^2}, \tag{5}$$

where $E_{0j} < E_g$ for free/unbounded Lorentz oscillators, and $G_f(E)$ is the set of the Gaussian oscillators [26,27]

$$G_f(E) = \sum_j A_j \left\{ \exp\left[-\left(\frac{E - E_{0j}}{C_j} \right)^2 \right] - \exp\left[-\left(\frac{E + E_{0j}}{C_j} \right)^2 \right] \right\} \tag{6}$$

(the Gaussian oscillators can be placed below as well as above E_g).

The real part of the dielectric function ε_1 for the TLLG oscillator model is obtained by the Kramers–Kronig integration of the ε_2 function described by Eq. (3):

$$\varepsilon_1(E) = \varepsilon_\infty + \frac{2}{\pi} P \int_{E_g}^{\infty} \frac{\xi \varepsilon_2(\xi)}{\xi^2 - E^2} d\xi, \tag{7}$$

where ε_∞ represents the value of real part of the dielectric function ε at infinite energy and it is an additional fitting parameter in the oscillator model, the P stands for the Cauchy principal part of the integral. The TLLG model is implemented in OLSA (Off-Line Spectral Analysis), a software package for the development and optimization of film dispersion models, available from KLA-Tencor Corporation (Milpitas, CA, U.S.A.).

3. Results and Discussion

3.1. Interfacial defects in SiO_2 layer

Figure 1 shows the imaginary part of the dielectric function ε_2 for ~20 Å thick gate oxide and its parameterization by the TLLG model with four Gaussian oscillators (no TL oscillators was used in that case since the oxide's optical absorption edge is outside our measurement range). These results were obtained from *ex situ* spectroscopic ellipsometry measurements performed at room temperature using research-grade rotating-compensator spectroscopic ellipsometer M-2000® from J.A. Woollam Co., Inc. in the spectral region of 192–1678 nm (0.74–6.47 eV) at several angles of incidence (50–75°). All ellipsometric measured data were analyzed using the wavelength point-by-point extraction procedure as well as the TLLG oscillator model which results in four sub-bandgap discrete absorption features with Gaussian line shapes located at 2.82, 3.24, 4.20, and 6.50 eV (Table 1). First absorption peak corresponds to a localized defect in Si/SiO_2 film system which has been observed

first by Price et al. [7] and most likely associated with a positively charged oxygen vacancy. Two other absorption features nearly coincide with the energies of critical points E_0' and E_2 of silicon (E_0'~3.30 eV, E_2~4.25 eV [28]; E_0'~3.320 eV, E_2~4.270 eV, E_1'~5.317 eV [29]; E_0'~3.316 eV, E_2~4.248 eV [30]). It is believed that the appearance of these absorption bands can be associated with inaccuracy of the model used for point-by-point data inversion [3]. The absorption band at ~6.5 eV has been previously detected [31–33] and attributed to a Si-Si-Si structure, an oxygen-deficiency related defect, in the oxide film.

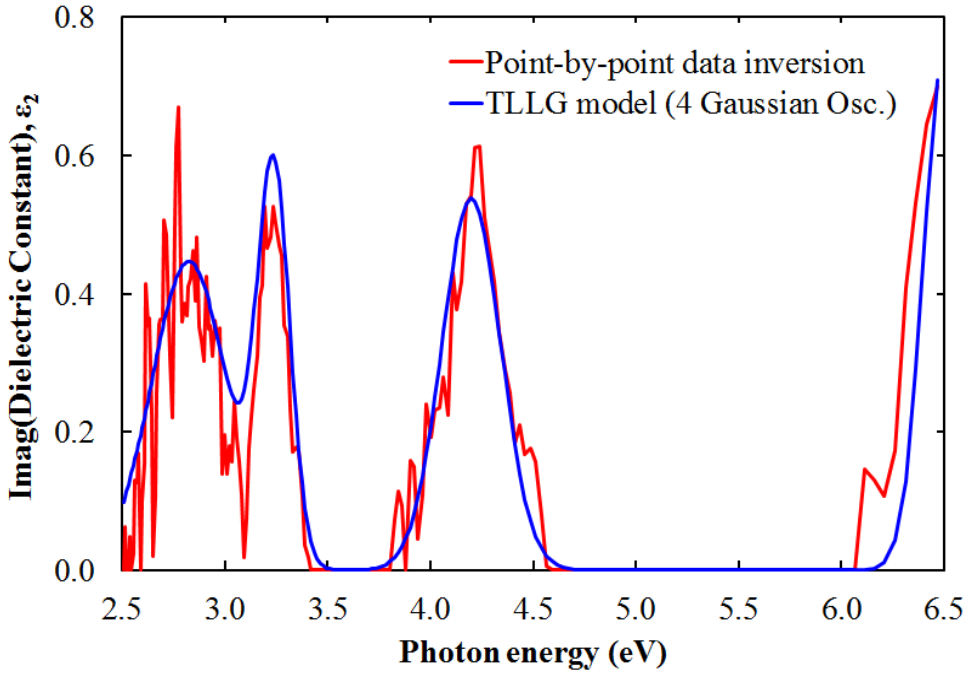

Figure 1. Imaginary part of the dielectric function ε_2 for ~20 Å thick gate oxide and its parameterization by the TLLG model with four Gaussian oscillators (no TL oscillators was used in that case since the oxide's optical absorption edge is outside our measurement range).

Table 1. TLLG model parameters for ~ 20 Å thick gate oxide.

Model parameter	Gaussian Oscillator #			
	1	2	3	4
A* (d.u.)	0.4467	0.5651	0.5385	0.7485
***E*$_0$ (eV)**	2.8249	3.2371	4.1995	6.5034
***C* (eV)**	0.2594	0.1115	0.2029	0.1441

*the abbreviation for dimensionless units

No prominent absorption features at 3.6 eV and 3.9 eV, observed in Ref. 7, as well as absorption peak at 4.75 eV, detected in Ref. 9 for the Si/SiO_2 stack, were observed in this study. Absence of those absorption features may be explained by many factors such as different substrate surface conditions or quality of the gate oxide layer.

3.2. Sub-bandgap absorption features in hafnium oxide (HfO_2) and hafnium aluminate (HfAlO)

Hf-based high-κ dielectric oxides are widely employed for a variety of applications (a replacement for SiO_2 as a gate insulator, transparent optical coatings with tunable electrical conductivity, high-κ dielectrics in capacitors, insulating barriers in tunnel junctions, planar waveguides and as an etch-stop layer for phase-shifting masks, etc.) in microelectronic, photovoltaic and optoelectronic industries. Multiple studies on the hafnium dioxide HfO_2 optical properties have reported the presence of an absorption feature 0.2–0.3 eV below the optical band-gap energy E_g and attributed this feature to the hafnium dioxide crystallinity or, in particular, to monoclinic phase of HfO_2 [1,2,8,14,15,34–41]. Similar sub-bandgap absorption feature has been also reported for atomic-layer-deposited (ALD) aluminum oxide Al_2O_3 [42].

Nguyen et al. [2] determined the energy parameters for high-quality HfO_2 and HfSiO films from vacuum-ultraviolet SE data by plotting the empirical expression $(n(E)\alpha(E)E)^{1/2}$ versus E and linearly extrapolating it to $(n(E)\alpha(E)E)^{1/2} = 0$ (the Tauc plot method), where n, α, and E are the index of refraction, the absorption coefficient, and the photon energy, respectively. The dielectric function ε was extracted by inverting the ellipsometric data at each wavelength ("point-by-point data inversion"). For the 400 Å thick ALD HfO_2 the following values have been obtained: $E_g = 5.80 \pm 0.05$ eV and $E_{def} = 5.60$ eV, where E_{def} is the "defect" feature energy (herein, the appearance of the sub-bandgap absorption feature).

Table 2. TLLG model parameters for 400 Å thick HfO_2 film.

Model parameter	Oscillator Type		
	TL #1	TL #2	Gaussian
***A* (eV)**	449.5	95.54	0.394 (d.u.)
***E*$_0$ (eV)**	6.140	7.131	5.935
***C* (eV)**	4.601	1.226	0.312
***E*$_g$ (eV)**	5.741	5.741	n/a

We applied the TLLG model to fit ε_2 spectrum extracted by Nguyen et al. [2]. Figure 2 shows the imaginary part of the HfO_2 dielectric function ε_2 and its parameterization by combination of two TL oscillators with Gaussian function. Table 2 summarizes the best-fit parameters for the 400 Å thick HfO_2 film. The TLLG model gives the following energy parameters: $E_g = 5.74$ eV, $E_{def} = 5.57$ eV. The value of energy bandgap parameter obtained from the TLLG model is similar to that from the Tauc plot method (as already pointed out by Di et al. [43] for the case of ordinary TL model). Thus, the TLLG model adequately describes the sub-band absorption features observed in HfO_2 thin films in contrast to Refs. 15, 38 where this specific shape absorption has been incorrectly associated with the exponential Urbach tail (as it was also previously noted by Franta et al. [44]).

Moreover, our results show a correlation between not only the energy band gap but also the bounded oscillators positions (E_{0j}), obtained from the TLLG model, to other important material properties such as composition, phase structure, doping, stress, etc. As an example, we applied the model to fit ε_2 spectrum for the hafnium aluminate (HfAlO) films with various Al concentration extracted by Nguyen et al. [45]. The best-fit parameters of TLLG model for the set of HfAlO thin films are listed in Table 3. Figure 3 shows a plot of the TLLG model energy parameters E_0 for two TL oscillators as well as E_g versus the aluminium concentration for the samples of the HfAlO thin

films. This relatively weak linear variation of E_g is consistent with the results reported in Ref. 46. Besides that, the position of one of the TL oscillators (first E_0 in our model) also linearly depends on the aluminium content and this relation can be considered as a quantitative measure for the characterisation of the HfAlO thin films using optical spectroscopic measurements. Note that the variation in oscillator position E_0 is even more pronounced than the increase in band-gap energy E_g (see Figure 3) (a little effect of Al on the band gap of HfO_2 was also reported in a few papers [47,48]).

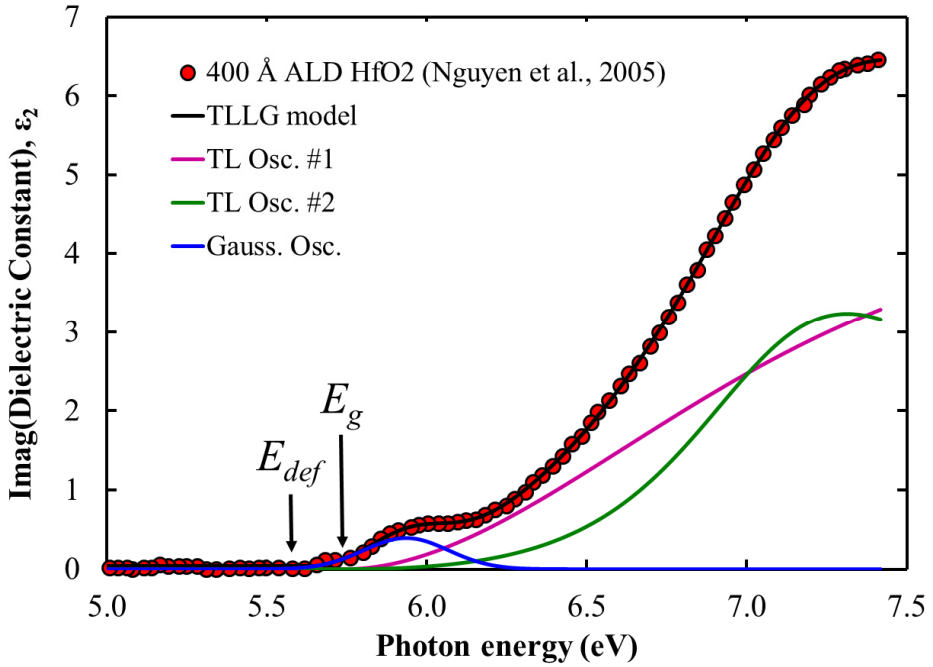

Figure 2. Imaginary part of the dielectric function ε_2 for 400 Å thick HfO_2 film (from Ref. 2) and its parameterization by the TLLG model with two TL oscillators and common E_g parameter plus single Gaussian oscillator.

Table 3. TLLG model parameters for the samples of HfAlO thin films.

Model parameter	Al concentration (at.%)		
	0.0	**13.2**	**45.5**
A_{TL1} (eV)	113.7	92.88	52.01
A_{TL2} (eV)	24.34	31.32	28.91
A_G (d.u.)	0.274	0.286	0.273
$E_{0\,TL1}$ (eV)	7.50	7.83	8.22
$E_{0\,TL2}$ (eV)	7.22	7.21	7.39
$E_{0\,G}$ (eV)	5.84	6.24	6.36
C_{TL1} (eV)	4.83	4.06	2.83
C_{TL2} (eV)	1.14	1.74	1.61
C_G (eV)	0.648	0.818	0.809
E_g (eV)	5.53	5.79	5.93

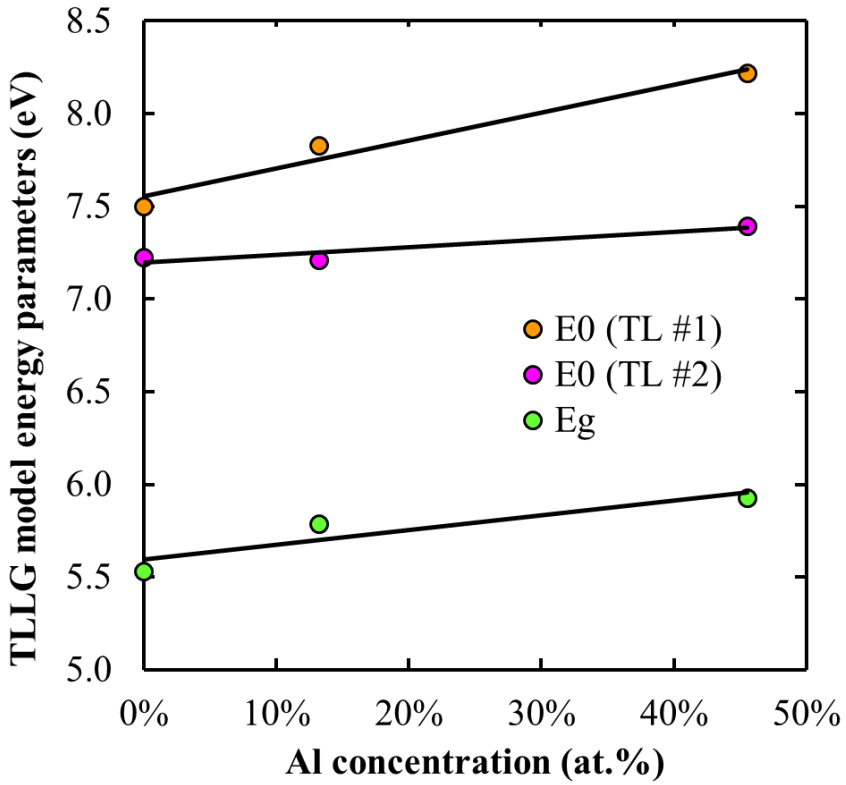

Figure 3. Variations of the TLLG model energy parameters E_0 and E_g vs. the aluminium concentrations for the samples of HfAlO thin films obtained by fitting the ε_2 spectrum (from Ref. 45). The solid lines are the linear trendlines.

3.3. Modeling of the UO_x dielectric function near the optical absorption edge

Uranium oxides are not only used in nuclear industry but due to their interesting electronic and electro-optical properties have been studied for other potential applications which include manufacturing of highly reflective multilayer mirrors for the extreme ultraviolet region, photo-anodes in photoelectrochemical cells for solar-assisted hydrogen production, efficient solar cells and fabrication of certain active electronic devices (a Schottky diode and a bipolar *p–n–p* transistor) [49,50,51]. The optical properties of the uranium oxide films deposited by magnetron sputtering were determined over different spectral ranges by spectroscopic ellipsometry in Refs. 52, 53. The UO_x dielectric functions in these references were obtained by applying the Drude–Lorentz model [52] and point-by-point data inversion [53] (the latter uses six different methods of the band gap determination based on linear extrapolation of various functional dependences for ε_2 and the absorption coefficient α).

Here we used the TLLG model to fit ε_2 spectrum extracted by He et al. [53]. A combination of two TL oscillators with common E_g and Lorentz function was used to fit the UO_x optical properties (Figure 4). Table 4 summarizes the best-fit parameters for ~1000 Å thick UO_x film. Using the TLLG model, the value of energy bandgap parameter was determined to be E_g = 2.59 eV which is slightly smaller than the value obtained by the Tauc plot method (E_g = 2.64 ± 0.02 eV, Ref. 53) and very close to the band-gap energy of 2.61 eV determined in Ref. 54 for α-UO_3, the α-phase of uranium

trioxide, a "non-traditional" semiconducting material. Note that the Lorentz function worked better than Gaussian one in fitting the broad sub-band feature below bandgap E_g.

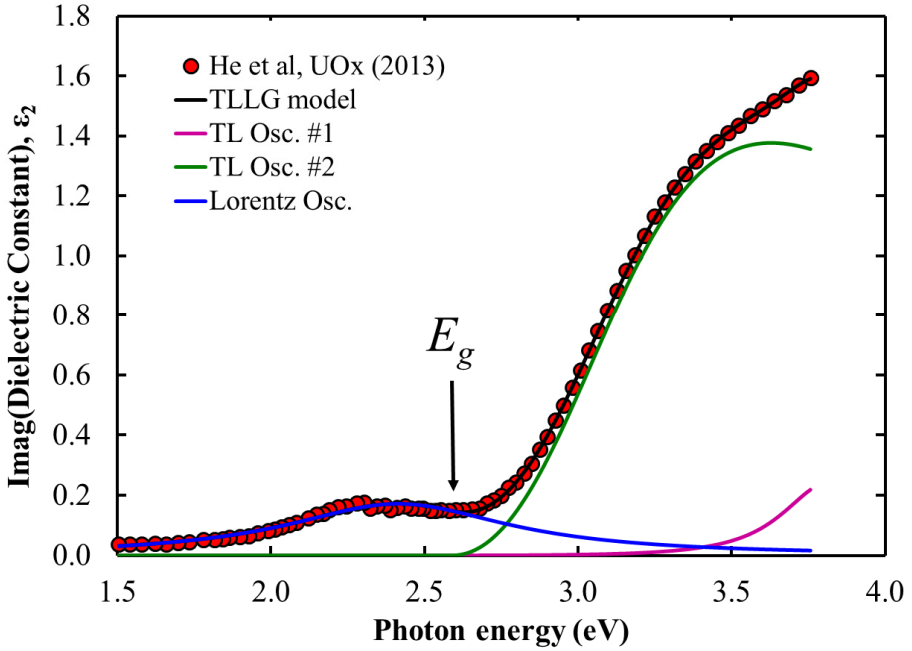

Figure 4. Imaginary part of the dielectric function ε_2 for ~1000 Å thick UOx film (from Ref. 53) and its parameterization by the TLLG model with two TL oscillators and common E_g parameter plus single Lorentz oscillator.

Table 4. TLLG model parameters for ~1000 Å thick UO_x film.

Model parameter	Oscillator Type		
	TL #1	TL #2	Lorentz
A (eV)	0.937	41.30	0.170 (d.u.)
E_0 (eV)	3.805	3.105	2.454
C (eV)	0.396	1.456	0.888
E_g (eV)	2.590	2.590	n/a

4. Conclusion

The physics-based parameterization of the dielectric functions of various materials is one of the most commonly used approaches in current optical metrology, in particularly, in spectroscopic ellipsometry. The reason is that a broad range of important material properties can be characterized based on physically meaningful parameters of the optical model for the dielectric function. One of the most widely used for amorphous materials is the Tauc-Lorentz oscillator model which, however, is not always correctly implemented and also explicitly neglects the absorption below the bandgap. In this paper, a modified Tauc-Lorentz dispersion model with common band-gap parameter E_g and possibility to represent reasonably the absorption features below the bandgap was applied to dielectric function parameterization near the optical absorption edge and sub-bandgap absorption

features in the Si/SiO_2 film system as well as in hafnium dioxide HfO_2 and uranium oxide UO_x thin films. The model is flexible enough to adequately portray the dielectric functions for a wide variety of materials. This should facilitate the study of process-induced defects and/or interface states in thin dielectric films as well as electronic excitations in thin organic films via spectroscopic measurements. The most obvious improvement of the proposed model would be replacement of separate unbounded Lorentz and Gaussian oscillators by a generalized Gauss-Lorentz dispersion model in which the oscillator broadening varies smoothly between Lorentzian and Gaussian types via adjustment of an additional shape parameter.

Acknowledgments

The authors wish to acknowledge support and collaboration among GLOBALFOUNDRIES and KLA-Tencor Corp.

Conflict of Interest

The authors declare that there are no conflicts of interest related to this study.

References

1. Takeuchi H, Ha D, King T-J (2004) Observation of bulk HfO_2 defects by spectroscopic ellipsometry. *J Vac Sci Technol A* 22: 1337–1341.
2. Nguyen NV, Davydov AV, Chandler-Horowitz D, et al. (2005) Sub-bandgap defect states in polycrystalline hafnium oxide and their suppression by admixture of silicon. *Appl Phys Lett* 87: 192903.
3. Price J, Lysaght PS, Song SC, et al. (2007) Identification of sub-band-gap absorption features at the HfO_2/Si(100) interface via spectroscopic ellipsometry. *Appl Phys Lett* 91: 061925.
4. Ferrieu F, Dabertrand K, Lhostis S, et al. (2007) Observation of HfO_2 thin films by deep UV spectroscopic ellipsometry. *J Non-Cryst Solids* 353: 658–662.
5. Price J, Lysaght PS, Song SC, et al. (2008) Observation of interfacial electrostatic field-induced changes in the silicon dielectric function using spectroscopic ellipsometry. *Phys Status Solidi A* 205: 918–921.
6. Price J, Bersuker G, Lysaght PS (2009) Identification of interfacial defects in high-κ gate stack films by spectroscopic ellipsometry. *J Vac Sci Technol B* 27: 310–312.
7. Price J, Bersuker G, Lysaght PS (2012) Identification of electrically active defects in thin dielectric films by spectroscopic ellipsometry. *J Appl Phys* 111: 043507.
8. Vasić R, Consiglio S, Clark RD, et al. (2013) Multi-technique x-ray and optical characterization of crystalline phase, texture, and electronic structure of atomic layer deposited $Hf_{1-x}Zr_xO_2$ gate dielectrics deposited by a cyclical deposition and annealing scheme. *J Appl Phys* 113: 234101.
9. Fan X, Liu H, Zhang X (2014) Identification of optimal ALD process conditions of Nd_2O_3 on Si by spectroscopic ellipsometry. *Appl Phys A* 114: 545–550.
10. Fan X, Liu H, Zhang X, et al. (2015) Optical characteristics of H_2O-based and O_3-based HfO_2 films deposited by ALD using spectroscopy ellipsometry. *Appl Phys A* 119: 957–963.

11. Collins RW, Ferlauto AS (2005) Optical physics of materials, In: Tompkins HG, Irene EA (Eds.), Handbook of Ellipsometry, Norwich: William Andrew Publishing/Noyes, 93–235.
12. Jellison GE Jr. (2005) Data analysis for spectroscopic ellipsometry, In: Tompkins HG, Irene EA (Eds.), Handbook of Ellipsometry, Norwich: William Andrew Publishing/ Noyes, 237–296.
13. Petrik P (2014) Parameterization of the dielectric function of semiconductor nanocrystals. *Physica B* 453: 2–7.
14. Cho YJ, Nguyen NV, Richter CA, et al. (2002) Spectroscopic ellipsometry characterization of high-κ dielectric HfO_2 thin films and the high-temperature annealing effects on their optical properties. *Appl Phys Lett* 80: 1249–1251.
15. Sancho-Parramon J, Modreanu M, Bosch S, et al. (2008) Optical characterization of HfO_2 by spectroscopic ellipsometry: Dispersion models and direct data inversion. *Thin Solid Films* 516: 7990–7995.
16. Jellison, Jr GE, Modine FA (1996) Parameterization of the optical functions of amorphous materials in the interband region. *Appl Phys Lett* 69: 371–373; Erratum: ''Parameterization of the optical functions of amorphous materials in the interband region'' [*Appl Phys Lett* 69, 371 (1996)], *idid*. 69: 2137.
17. Ferlauto AS, Ferreira GM, Pearce JM, et al. (2002) Analytical model for the optical functions of amorphous semiconductors from the near-infrared to ultraviolet: Applications in thin film photovoltaics. *J Appl Phys* 92: 2424–2436.
18. Ferlauto AS, Ferreira GM, Pearce JM, et al. (2004) Analytical model for the optical functions of amorphous semiconductors and its applications for thin film solar cells. *Thin Solid Films* 455–456: 388–392.
19. Foldyna M, Postava K, Bouchala J, et al. (2004) Model dielectric functional of amorphous materials including Urbach tail, In: Pistora J, Postava K, Hrabovsky M, et al. (Eds.), Microwave and Optical Technology 2003, Ostrava, Czech Republic, August 11–15, 2003, SPIE Proc. 5445: 301–305.
20. Falahatgar SS, Ghodsi FE (2013) A developed model for the determination of the dielectric function for some absorbing thin films using pseudo-Urbach tail. *Physica B* 412: 4–11.
21. Price J, Hung PY, Rhoad T, et al. (2004) Spectroscopic ellipsometry characterization of $Hf_xSi_yO_z$ films using the Cody–Lorentz parameterized model. *Appl Phys Lett* 85: 1701–1703.
22. Kamineni VK, Hilfiker JN, Freeouf JL, et al. (2011) Extension of far UV spectroscopic ellipsometry studies of high-κ dielectric films to 130 nm. *Thin Solid Films* 519: 2894–2898.
23. Mei JJ, Chen H, Shen WZ, et al. (2006) Optical properties and local bonding configurations of hydrogenated amorphous silicon nitride thin films. *J Appl Phys* 100: 073516.
24. Eiamchai P, Chindaudom P, Pokaipisit A, et al. (2009) A spectroscopic ellipsometry study of TiO_2 thin films prepared by ion-assisted electron-beam evaporation. *Curr Appl Phys* 9: 707–712.
25. Avci N, Smet PF, Poelman H, et al. (2009) Characterization of TiO_2 powders and thin films prepared by non-aqueous sol–gel techniques. *J Sol-Gel Sci Technol* 52: 424–431.
26. Peiponen K-E, Vartiainen EM (1991) Kramers-Kronig relations in optical data inversion. *Phys Rev B* 44: 8301–8303.
27. De Sousa Meneses D, Malki M, Echegut P (2006) Structure and lattice dynamics of binary lead silicate glasses investigated by infrared spectroscopy. *J Non-Cryst Solids* 352: 769–776.
28. Jellison, Jr. GE, Modine FA (1983) Optical functions of silicon between 1.7 and 4.7 eV at elevated temperatures. *Phys Rev B* 27: 7466–7472.

29. Lautenschlager P, Garriga M, Viña L, et al. (1987) Temperature dependence of the dielectric function and interband critical points in silicon. *Phys Rev B* 36: 4821–4830.
30. Vineis CJ (2005) Complex dielectric function of biaxial tensile strained silicon by spectroscopic ellipsometry. *Phys Rev B* 71: 245205.
31. Awazu K, Kawazoe H, Saito Y, et al. (1991) Structural imperfections in silicon dioxide films identified with vacuum ultraviolet optical absorption measurements. *Appl Phys Lett* 59: 528–530.
32. Awazu K, Kawazoe H, Muta K-i (1991) Optical properties of oxygen-deficient centers in silica glasses fabricated in H_2 or vacuum ambient. *J Appl Phys* 70: 69–74.
33. Terada N, Haga T, Miyata N, et al. (1992) Optical absorption in ultrathin silicon oxide films near the SiO_2/Si interface. *Phys Rev B* 46: 2312–2318.
34. Aarik J, Mändar H, Kirm M, et al. (2004) Optical characterization of HfO_2 thin films grown by atomic layer deposition. *Thin Solid Films* 466: 41–47.
35. Lucovsky G, Zhang Y, Luning J, et al. (2005) Intrinsic band edge traps in nano-crystalline HfO_2 gate dielectrics. *Microelectron Eng* 80: 110–113.
36. Hoppe EE, Sorbello RS, Aita CR (2007) Near-edge optical absorption behavior of sputter deposited hafnium dioxide. *J Appl Phys* 101: 123534.
37. Ferrieu F, Dabertrand K, Lhostis S, et al. (2007) Observation of HfO_2 thin films by deep UV spectroscopic ellipsometry. *J Non-Cryst Solids* 353: 658–662.
38. Martínez FL, Toledano-Luque M, Gandía JJ, et al. (2007) Optical properties and structure of HfO_2 thin films grown by high pressure reactive sputtering. *J Phys D: Appl Phys* 40: 5256–5265.
39. Hill DH, Bartynski RA, Nguyen NV, et al. (2008) The relationship between local order, long range order, and sub-band-gap defects in hafnium oxide and hafnium silicate films. *J Appl Phys* 103: 093712.
40. Park J-W, Lee D-K, Lim D, et al. (2008) Optical properties of thermally annealed hafnium oxide and their correlation with structural change. *J Appl Phys* 104: 033521.
41. Bersch E, Di M, Consiglio S, et al. (2010) Complete band offset characterization of the HfO_2/SiO_2/Si stack using charge corrected x-ray photoelectron spectroscopy. *J Appl Phys* 107: 043702.
42. Xu K, Sio H, Kirillov OA, et al. (2013) Band offset determination of atomic-layer-deposited Al_2O_3 and HfO_2 on InP by internal photoemission and spectroscopic ellipsometry. *J Appl Phys* 113: 024504.
43. Di M, Bersch E, Diebold AC, et al. (2011) Comparison of methods to determine bandgaps of ultrathin HfO_2 films using spectroscopic ellipsometry. *J Vac Sci Technol A* 29: 041001.
44. Franta D, Ohlídal I, Nečas D, et al. (2011) Optical characterization of HfO_2 thin films. *Thin Solid Films* 519: 6085–6091.
45. Nguyen NV, Han J-P, Kim JY, et al. (2003) Optical properties of jet-vapor-deposited TiAlO and HfAlO determined by vacuum utraviolet spectroscopic ellipsometry, In: Seiler DG, Diebold AC, Shaffner TJ, et al. (Eds.), Characterization and Metrology for ULSI Technology 2003, Austin, TX, U.S.A., March 24–28, 2003, AIP Conf. Proc. 683: 181–185.
46. Nguyen NV, Sayan S, Levin I, et al. (2005) Optical band gaps and composition dependence of hafnium–aluminate thin films grown by atomic layer chemical vapor deposition. *J Vac Sci Technol A* 23: 1706–1713.
47. Wang XF, Li Q, Egerton RF, et al. (2007) Effect of Al addition on the microstructure and electronic structure of HfO_2 film. *J Appl Phys* 101: 013514.

48. Park TJ, Kim JH, Jang JH, et al. (2010) Reduction of electrical defects in atomic layer deposited HfO_2 films by Al doping. *Chem Mater* 22: 4175–4184.
49. Sandberg RL, Allred DD, Lunt S, et al. (2004) Optical properties and application of uranium-based thin films for the extreme ultraviolet and soft x-ray region, In: Soufli R, Seely JF (Eds.), Optical Constants of Materials for UV to X-Ray Wavelengths, Denver, CO, U.S.A., August 2, 2004, SPIE Proc. 5538: 107–118.
50. Meek TT, von Roedern B (2008) Semiconductor devices fabricated from actinide oxides. *Vacuum* 83: 226–228.
51. Kruschwitz CA, Mukhopadhyay S, Schwellenbach D, et al. (2014) Semiconductor neutron detectors using depleted uranium oxide, In: Burger A, Franks L, James RB, et al. (Eds.), Hard X-Ray, Gamma-Ray, and Neutron Detector Physics XVI, San Diego, CA, U.S.A., August 17, 2014, SPIE Proc. 9213: 92130C-1–92130C-9.
52. Chen Q, Lai X, Bai B, et al. (2010) Structural characterization and optical properties of UO_2 thin films by magnetron sputtering. *Appl Surf Sci* 256: 3047–3050.
53. He H, Andersson DA, Allred DD, et al. (2013) Determination of the insulation gap of uranium oxides by spectroscopic ellipsometry and density functional theory. *J Phys Chem C* 117: 16540–16551.
54. Khilla MA, Rofail NH (1986) Optical absorption edge of uranium trioxide phases: Part I. *Radiochim Acta* 40: 155–158.

AIMS Press